Design, Modeling and Test of a Novel Speed Bump Energy Harvester

Prakhar Todaria , Lirong Wang, Abhishek Pandey, James O'Connor, David McAvoy,

Terence Harrigan, Barbara Chernow, Lei Zuo*

ABSTRACT

Speed bumps are commonly used to control the traffic speed and to ensure the safety of pedestrians. This paper proposes a novel speed bump energy harvester (SBEH), which can generate large-scale electrical energy up to several hundred watts when the vehicle drives on it. A unique design of the motion mechanism allows the up-and-down pulse motion to drive the generator into unidirectional rotation, yielding time times more energy than the traditional design. Along with the validation of energy harvesting, this paper also addresses the advantages of this motion mechanism over the traditional design, using physical modeling and simulation. Up to 200 watts electrical peak power in one phase of three-phase generator during in-field test can be regenerated when a sedan passage car passes through the SBEH prototype at 2 km/h.

Keywords: Speed Bump, Energy Harvester, Vehicle Dynamics

1 INTRODUCTION

A speed bump is basically an elevated profile placed across the road, usually 3-5" high and various length[1]. Speed bumps are installed in the areas where human-traffic interaction is relatively high to reduce the risk of accidents[2]. The speed reduction of vehicle while encountering speed bumps not only has influence to the ride comfort of driver/passengers, but also results in huge kinetic energy loss at the same time. Various attempts have been made to improve the driver/passengers comfort while passing through speed bumps by optimizing the shape and height of the bumps[3]–[6]. There have also been many attempts to harvest energy from speed bumps by means of piezoelectric or electromagnetic devices, such as the literature [7]–[10]. The harnessed energy is usually small with only impulse voltage at the level of 20V voltages or less in those cases.

This paper investigate an energy harvesting technology via speed bump to regenerate large-scale energy when a vehicle encounters the speed bump. The SBEH is designed based on a unique highly efficient energy conversion mechanism, which we called Mechanical Motion Rectifier (MMR). The MMR converts both down and up pulse motions of speed bump into one direction rotation of the electrical generator to produce electrical power. It has unique advantage over the traditional electromagnetic generator where the movement of the shaft is limited due to the pulse-like motion and thus cannot provide the continuous and unidirectional rotation to the input shaft of the generator. A prototype is fabricated and tested to approve the effectiveness of energy harvesting. Modelling of SBEH and its interaction with vehicle are investigated. Simulation results are provided in comparison with the traditional design. Experimental results also reveal the energy harvesting mechanism and design principle of the energy harvesting speed bump.

2 DESIGN AND FABRICATION OF ENERGY HARVESTER

The objective to design a SBEH is to regenerate electrical energy from the pulse motion of speed bump excited by the impact of the passing vehicles. The designed SBEH can conveniently replace the existing speed bumps on the road as a cost-effective power supply to obtain electricity for road-side devices. The SBEH is mainly composed of two parts: energy harvesting unit and speed bump cover unit, as shown in Figure 1. The speed bump cover unit includes a speed bump cover with the geometrical profile similar as that of conventional speed bump, a base plate, springs & linear bearing to support speed bump load on a cavity under the road surface. Energy harvester unit is enclosed in the harvester housing for water proof. A connector connects the harvester with speed bump cover and works as an input to the harvester. The movement of the connector will cause the translational motion in the racks, which in turn will rotate the generator shaft inside the harvester to generate electrical power. The design detail is introduced in the following sub-sections.

*Note: This project is partially supported by SUNY Sustainability Fund. This report is reprint of a paper published in the Proceedings of 2015 SPIE Smart Structures/NDE Conference, March 8-12, 2015,San Diego, CA (Contact: lei.zuo@stonybrook.edu)

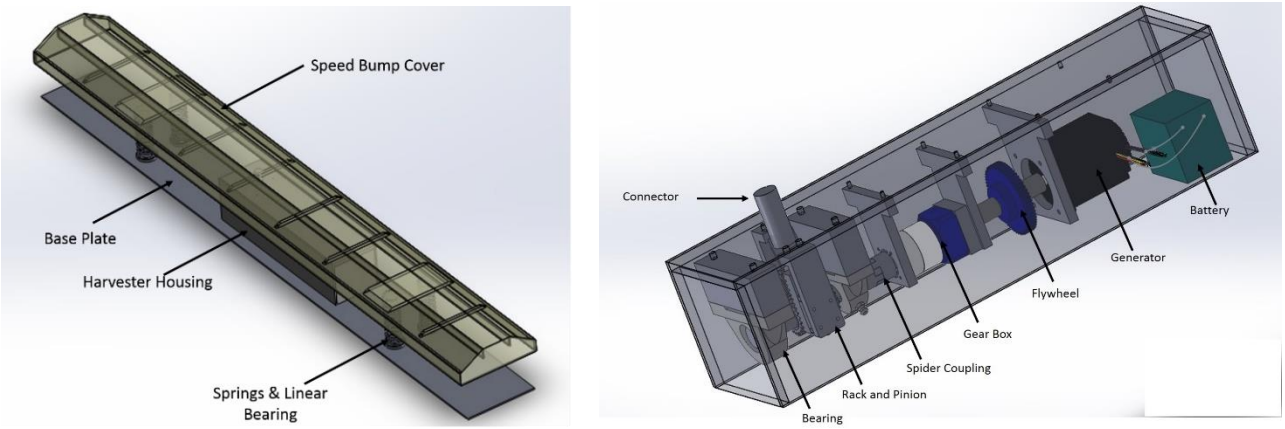

Figure 1. Illustration of SBEH units. Left: Speed bump cover unit. Right: Energy harvesting unit

2.1 Design of energy harvester unit

Energy harvester is the kernel part of SBEH, which is formed of energy conversion unit. It includes two sets of racks and pinions, one shaft, two one-way clutches between the shaft and pinion gears, a gearbox, a flywheel, a rotational generator, and energy storage device such as battery, as illustrated in Figure 1. The schematics of energy conversion mechanism, as shown in Figure 2, which is called the mechanical motion rectifier (MMR)[11], by which the linear translational motions of two racks are converted to the rotational motion with the engagement and disengagement of the two one-way clutches. The two racks are connected with speed bump cover via the connector. When the two racks move with the speed bump cover vertically, the two pinions will rotate with the movement of racks. However, the two one-way clutches inside the pinions are installed in such a way that only one of the two clutches is engaged at an instant time to drive the shaft. When a vehicle rolls over the speed bump cover, the speed bump cover and racks are first pressed down and. During this process, the first one-way clutch is engaged and drives the shaft meanwhile, the second one-way clutch is disengaged. After the tire rolls over, the speed bump and racks will move upwards under the spring force. The second one-way clutch is engaged to drive coupling shaft and the first one-way clutch is disengaged. The engagement and disengagement between the pair of one-way clutches result in the coupling shaft to be driven in the same direction, irrespective of the direction of the movement of racks. This is the working principle of the proposed mechanical motion rectifier, which is similar as the electrical voltage rectifier using center-tapped transformer. Since the rotational speed obtained by the linear motion of rack is not so high, a gear box is used to speed up the generator to its rated speed for energy conversion efficiency.

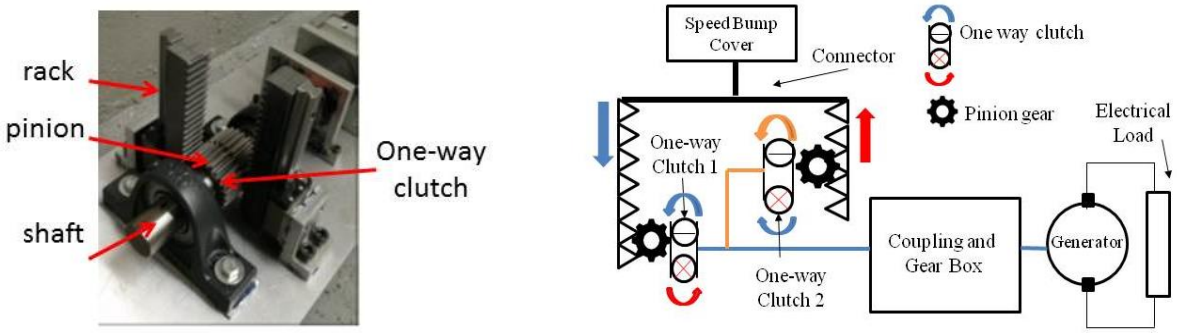

Figure 2. Mechanism of energy harvesting. Left: rack and pinion. Right: schematics of MMR

Furthermore, when the racks hit the motion limits and stop moving, both one-way clutches will be disengaged and the generator will continue rotating unless all the kinetic energy stored into rotary inertia (including the shaft, gear box, and the generator inertia) is converted into electricity. Additional flywheel can be added to increase the rotary inertia. An energy storage device such as battery and an electrical circuit is connected with the output of the generator to store the energy. A prototype according to the harvest design is fabricated as illustrated in Figure 1 (right).

2.2 Design of speed bump cover unit

Speed bump cover is supposed to carry the vehicle load and support the impact shock from vehicle tires. Therefore, the cover had to be robust enough to endure both large static load and dynamic impact. The profile of speed bump is important since it influences the interaction between vehicle and speed bump. In this research, a general trapezoid topology of traditional speed bump is adopted and simplified as show in Figure 1. In the inner part of speed bump cover, cross ribs between the two slanted sides and along the length direction are introduced to enhance the cover strength. The height of the cover was kept at 3.5 inches overall so that with a stroke of 2 inches the speed bump remains a height one inch above the ground when completely pushed down. The overall length of the bump was kept so that the vehicle of maximum axle length could be covered under the range of its application. The fabricated speed bump cover unit is as shown in Figure 3, which is made by material of iron with thickness 0.2 inches on all the sides. The total weight is around 150 kg or 330 lb.

Figure 3. Speed bump cover unit fabricated. Left: linear bearing, springs and mounting arrangements. Right: fabricated speed bump cover

As shown in Figure 3, four spring and four linear bearings are used to support and guide the speed bump cover on a base plate placed on the ground. Besides, the spring has function to provide rebounding force to speed bump so that it can recover its original position when there is no load on it. Linear bearings and stanless steel shafts are used to guide the speed bump cover which are supposed to be moved in vertical direction only. When the spring are compressed down, the cover connector will drive the racks inside the harvester, which can rotate the generator to produce power. When the speed bump cover is rebounded, we can expect the generator to produce power by harvesting the potential energy stored in springs. In order to be able to harvest more energy during this rebounding process, springs of high stiffness,742 lb/in , and long compression length 3.6 in were used. The springs are also preloaded at 5% displacement or total 297 lb force in addition to the static weight so that the speed bump can rebound quickly under the damping force induced by the harvester. In such design, electrical power generation can take place twice during a stroke. Moreover, the rebound time to its original position has to be less than the time when the rear axle of vehicle hits the speed bump.

The time for speed bump to rebound to its original position can be estimated by a quarter period of time according to its natural frequency. The natural frequency of speed bump can be expressed as

$$f_n = \sqrt{\frac{k}{(m_b + m_e)}} \tag{1}$$

Where f_n, k, m_b, and m_e will be the natural frequency of speed bump, spring stiffness, mass of speed bump and the equivalent mass of energy harvester which will be introduced in detail in Section 3.1. Assuming that the time between the front and rear axles of vehicle passing through the speed bump is T_v, then

$$\frac{1}{(4 \cdot f_n)} \leq \frac{1}{f_v} = T_v \tag{2}$$

Substitute Equation (1) into (2),

$$k \geq \frac{(m_b + m_e)}{T_v^2 16} \tag{3}$$

The time T_v , can be calculated according to vehicle speed and axle distance. Moreover, larger the equivalent mass of harvester, larger stiffness of the spring should be. Since the rebounding force of the spring is large, the upward limitation (stop) should be designed to prevent the whole speed bump cover to exceed the maximum height of linear bearing and damage the harvester.

3 MODELLING OF SBEH AND ITS INTERACTION WITH VEHICLE MODEL

This section presents the modelling of speed bump harvester to reveal its working mechanism and its interaction with vehicle passing through. Unlike the conventional speed bumps which give a fixed road profile to the vehicle, this energy harvesting speed bump design will move up and down and has dynamic interaction with the vehicle. To simplify the analysis, it is assumed that the vehicle passes the SBEH with a constant velocity of *V*, and thus the horizontal velocity of its tire is the same as that of vehicle velocity *V*. Moreover, only the vertical vibrations of both SBEH and vehicle are considered.

3.1 Modeling of SBEH

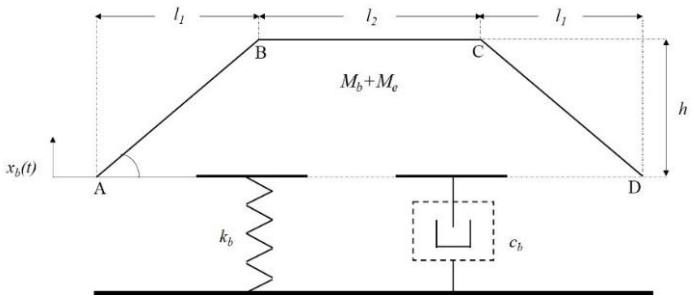

Figure 4. SBEH model

The energy harvester unit with MMR mechanism, when neither one-way clutches is disengaged, can be model as an equivalent mass and a damper according our previous research [12] and it is illustrated in Figure 4. Here the equivalent mass can be expressed in terms of the following equation

$$M_e = \frac{J_p + J_c + n^2 J_m}{r^2} \tag{4}$$

Where, J_p, J_c and J_m are the inertia of pinion gears, coupling shaft and generator respectively. The n is the gear ratio of gear box and R is the radius of the pinion gear. This equivalent mass is the inertial mass which will resist the motion of the bump cover in the beginning. So M_e can be added to the mass of the speed cover considering it to be placed at the end of the rack. The damping in energy harvester unit includes two kinds of damping, the mechanical damping C_m caused by the friction of mechanical devices in the racks and pinions, coupling shaft, gearbox, generator and electrical damping C_e caused by internal resistance and electrical load on generator. The electrical damping can be indicated as the following equation [12]

$$C_e = \frac{K_t K_g n^2}{(R_i + R_e) r^2} \tag{5}$$

where, K_t, K_g and R_i and are torque constant, voltage constant and internal resistance of the generator and R_e is the external load resistance connected to the output from the generator. The movement of the speed bump cover unit is defined as x_b in vertical direction, as shown in Figure 4. The speed bump cover is treated as one mass-spring vibration

system with M_b being the mass of the speed bump cover, K_b being the total stiffness of the four supporting springs. The maximum vertical displacements of x_b in both downwards and upwards directions are limited by the stoppers which stops the movement of the speed bump cover. Therefore, the maximum displacement speed bump can achieve is ' $x_{b\max}$ '. The profile of the speed bump is described by geometrical parameters of distance parameters l_1 (4.33 in), l_2 (5 in) and height h (3.5 in) as shown in Figure 4. The whole SBEH model is built up as one-mass vibration system by integrating the model of speed bump cover with that of harvester by attaching the equivalent mass and damping. Considering the working process of SBEH, its modeling can be analyzed in three stages.

Stage 1: (Downward stroke before the speed bump cover reaches $x_{b\max}$). During this process, the one-mass system can be expressed as one degree of freedom (DOF) with the following equation

$$(M_b + M_e)\ddot{x}_b + C_b\dot{x}_b + K_b(x_b - x_0) = 0 \tag{6}$$

Where (M_b + M_e) is the total mass of the sum of the speed bump cover and the equivalent mass of harvester; $\ddot{x}_b$ and $\dot{x}_b$ are the vertical acceleration and velocity respectively. The damping C_b is represented as a sum of equivalent electrical damping of the harvester and the mechanical or structural damping caused by the moving parts and their misalignment. For simplification, the structural damping ratio of 10% has been assumed for the harvester. Thus the total damping can be expressed as

$$C_b = C_e + C_m \tag{7}$$

In Eq. (6), say, $F_p = K_b x_0$, then Eq. (6) can be rewritten as,

$$(M_b + M_e)\ddot{x}_b + C_b\dot{x}_b + K_b x_b = F_p \tag{8}$$

Stage 2: (After speed bump reaches its bottom limit). When the speed bump cover reaches its bottom limit, it cannot move down further. Thus, when the displacement of the speed bump reaches the maximum limit, $x_{b\max}$, the dynamic equations , in this case, will follow the total disengagement case.

Total disengagement: Point to be noted here is that the coupling between the speed bump harvester and the speed bump cover depends on the velocity difference between the rotational speed of pinion ω driven by the instantaneous translational velocity of the speed bump cover of $\dot{x}_b$. If $\dot{x}_b / R \geq \omega$, the one-way clutches are engaged, and the SBEH rebounds by as the one-mass vibration system whose dynamic equation can be expressed as Eq (9), But if $\dot{x}_b / R < \omega$, that is, the generator speed is higher than the rotational speed of pinion, both one-way clutches are disengaged, and the speed bump energy harvester is separated from the speed bump cover unit. That is, the equivalent mass and damping of harvester no longer need not to be attached to the model of speed bump cover until they resume in the state of engagement. Hence, the one-mass vibration system of speed bump with the preload, can be expressed as,

$$M_b\ddot{x}_b + K_b x_{b\max} = F_p \tag{9}$$

Where $x_{b\max}$ is the maximum stroke of the speed bump cover. And the dynamic equation of energy harvester when both the one-way clutches are disengaged can be expressed as

$$M_e\ddot{\theta} + C_b\dot{\theta} = 0 \tag{10}$$

Where $\ddot{\theta}$ and $\dot{\theta}$ are the angular acceleration and velocity of the shaft after disengagement. This is also true for stage 1 if we consider that during the beginning of the stage 1 the system is totally disengaged. However, the difference will be

only with the value of x_b which will not be $x_{b\max}$. This case is possible if the vehicle velocity is high and the generator s haft is still running when the rear axle of the vehicle hits the bump again for the second stroke.

Stage 3: (Rebounding process when the vehicle tires are rolling out of the speed bump cover). When the vehicle tire move out of the speed bump cover, the speed bump cover will rebound as the one-mass vibration system under the spring force of F_p, and the dynamic equation returns to Eq. (8), if engaged, or to Eq. (9) if still disengaged.

Stage 4: (After speed bump reaches the upper limit after rebounding). This case is similar to stage 2 case. If during the stage 3, we assume the state of the system is engaged, then after the bump hits the upper hard stop, the harvester will again go to the total disengagement state as described in stage two special case of total disengagement. In that case, $x_b = 0$ and again the dynamics of harvester will be described by Eq. (10).

3.2 Vehicle Modeling and its interaction with SBEH model

3.2.1 Quarter Vehicle Model

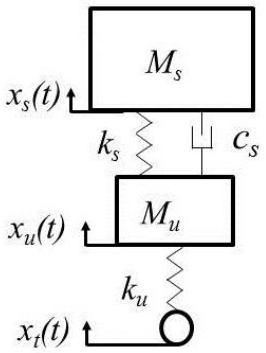

Figure 5. Axle car model

A quarter vehicle model from reference [13] is adopted in this research as illustrated in Figure 5. Only the vertical vibration of the vehicle is considered in this research. The quarter vehicle model is a two-mass vibration system with body mass of M_s and unspring mass of M_u. The vertical displacement of sprung and un-sprung mass is represented as x_s and x_u respectively. The stiffness and damping of the suspension system are described as K_s and C_s respectively and the stiffness of tire is indicated as K_u and the damping of tire is neglected due to be smaller than that of both suspension and speed bump. The two-mass vibration system can be expressed as the following two equations,

$$M_s\ddot{x}_s + C_s(\dot{x}_s - \dot{x}_u) + K_s(x_s - x_u) = 0 \tag{11}$$

$$M_u\ddot{x}_u - C_s(\dot{x}_s - \dot{x}_u) - K_s(x_s - x_u) + K_u(x_u - x_t) = 0 \tag{12}$$

Where $\ddot{x}_s$ and $\ddot{x}_u$ are the vertical accelerations of sprung and un-sprung mass respectively, $\dot{x}_s$ and $\dot{x}_u$ are the vertical velocity of the sprung and the un-sprung mass respectively. Here x_t is the movable displacement boundary input. x_t will be influenced by the position of tire and speed bump cover stroke. It can be analyzed in three stages as shown in Fig. 6.

Section I: Tire position is located between A and B as illustrated in Figure 6 (a). The vertical velocity of the tire can be synthesized in terms of horizontal velocity of the vehicle tire V and speed bump vertical velocity $\dot{x}_b$

$$\dot{x}_t = V\tan(\theta) - \dot{x}_b \tag{13}$$

Where θ is the angle between the slope of the cover and ground.

Section II: Tire position is located between B and C as illustrated in Figure 6 (b). When vehicle tires reach point B on the speed bump, the profile input becomes zero as $\theta = 0$. Thus, the tire velocity in vertical direction becomes,

$$\dot{x}_t = -\dot{x}_b \tag{14}$$

Section III: Tire position is located between C and D as illustrated in Figure 6 (c). When vehicle tires cross the point C on the profile of the speed bump, the tire contact points begins to go down the slope of the speed bump. In that case θ will be negative and Eq. (13) will change to

$$\dot{x}_t = -V \cdot \tan(\theta) - \dot{x}_b \tag{15}$$

By differentiating Eq. (13-15), we achieve another state as $\ddot{x}_t = -\ddot{x}_b$.

3.2.2 Dynamics of SBEH with MMR and its interaction with Quarter Vehicle Model

Although, both the systems have their individual dynamics, when they come in contact they behave as a three- of four-body mass system (depending on the engagement or disengagement of the generator). Hence, the overall system can be represented in terms of three equations of decoupled masses when they come in contact. Governing equations of the overall system can be written as

$$M_s\ddot{x}_s + C_s(\dot{x}_s - \dot{x}_u) + K_s(x_s - x_u) = 0 \tag{16}$$

$$M_u\ddot{x}_u - C_s(\dot{x}_s - \dot{x}_u) - K_s(x_s - x_u) + K_u(x_u - x_t) = 0 \tag{17}$$

$$(M_b + M_e)\ddot{x}_b - C_b\dot{x}_b - K_b x_b - K_u(x_s - x_t) = F_p - F_g \tag{18}$$

When a vehicle is passing through the SBEH, the interaction between vehicle and SBEH is much more complex due to the moving interactive boundary condition between the tire and the speed bump cover profile as described in the previous section. As shown in Figure 6, SBEH-Vehicle interaction can be regarded as a three-mass vibration system with governing Eqs. (16-18) added with another state described by Eqs. (13-15)

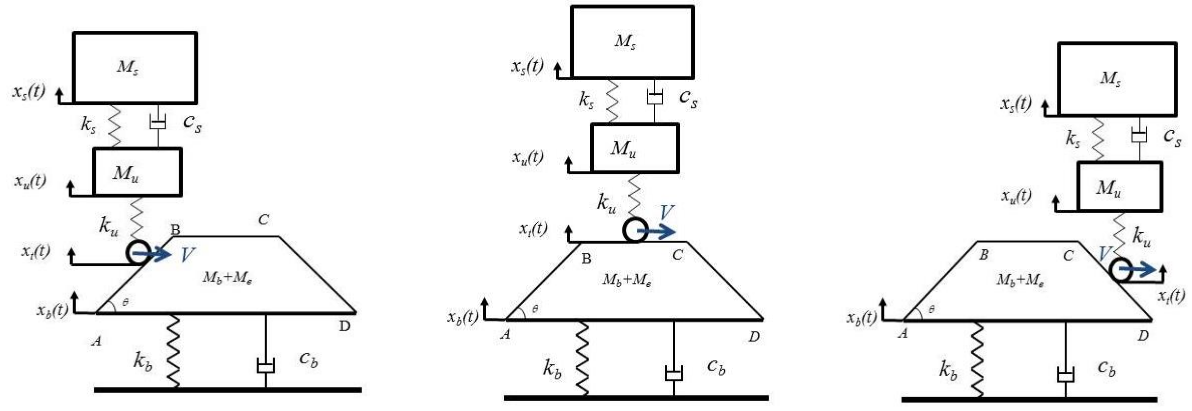

(a) (b) (c)

Figure 6. Interaction between SBEH model and vehicle model. (a) Vehicle is climbing on SBEH. (b) Vehicle is passing on top of SBEH. (c) Vehicle is going down the SBEH

When the two-mass vehicle model is made to interact with SBEH model, the vehicle weight of $F_g = Mg$ exerted on the speed bump cover vertically downwards. Here, M is the vehicle's overall mass and g the gravity acceleration.. Such a three-mass vibration system can be simplified and derived by synthesizing the SBEH model with the quarter vehicle but since the entire front axle will roll on the speed bump, we can double quarter vehicle model parameters i.e. double the sprung and un-sprung mass, double the suspension and tire stiffness and damping. Considering the three working stages of SBEH, the interaction between SBEH and vehicle can be analyzed as the following three stages.

(1) Before the speed bump cover reaches the bottom limit: During this process, the movement of the speed bump cover drives the rack via connector which in turn rotates the pinions. During this phase, the rotational speed of the coupling shaft will be slower than the speed of pinion therefore the one-way clutch will engaged as described in section 3.1 with Eq. (8).

$$(M_b + M_e)\ddot{x}_b + C_b\dot{x}_b + K_b x_b - K_u(x_u - x_t) = F_p - F_g \tag{19}$$

At the same time, vehicle works in a two-mass system as described by Eq. (12-13).

(2) After the speed bump reaches the bottom limit: When the speed bump cover reaches its hard stop, speed bump cannot move further and is stationary. At this moment, dynamic equation of SBEH is switched and under the influence of static vehicle load, F_g, following equation will command the system

$$M_b\ddot{x}_b + K_b x_{b\max} = F_p - F_g \tag{20}$$

At the same time, the movable displacement boundary input to vehicle model will not change because $x_b = x_{bmax}$, and the profile of speed bump cover will act as an fixed input to vehicle as the conventional speed bump. x_t will be the speed bump profile input to the vehicle model, which is the same as the tire rolling on the traditional speed bump with fixed boundary displacement input of speed bump profile. At this time, the SBEH vibration system and vehicle system has no interaction. Again, as in described in section 3.1, if $\dot{x}_b / R < \omega$, that is, the generator speed is higher than the rotational speed of pinion, one-way clutches are disengaged, and the speed bump energy harvester is separated from the speed bump cover unit. That is, the equivalent mass and damping of harvester need not to be attached to attach to the model of speed bump cover. The one-mass vibration system of speed bump with the preload, can be expressed as,

$$M_b\ddot{x}_b + K_b x_{b\max} = F_p - F_g \tag{21}$$

Where $x_{b\max}$ is the maximum stroke of the speed bump cover. Thus, $K_b x_{b\max}$ will always be constant. And the dynamics equation of energy harvester when both the one-way clutches are disengaged

$$M_e\ddot{x}_b + C_b\dot{x}_b = 0 \tag{22}$$

(3) Rebounding process when vehicle tires roll out of the speed bump cover: Since the vehicle weight is much large than the supporting force provided by the four springs of SBEH, the rebounding process only occurs when the vehicle tire move out of the speed bump cover when there is no interaction between speed bump and vehicle. Hence, as described in section 3.1, dynamic equation under the influence of static mass of the vehicle can be expressed as,

$$(M_b + M_e)\ddot{x}_b + C_b\dot{x}_b + K_b x_b = F_p - F_g \tag{23}$$

3.2.3 Dynamics of SBEH without MMR

To compare the influence of energy harvester with MMR to the dynamics of the interaction between speed bump and vehicle, a SBEH model where the rack and pinion is simple connected with the traditional electromagnetic generator

without the MMR mechanism. Equations of the quarter car model will remain the same. However, the speed bump model in the three mass-spring vibration system can be described as the followings.

(1) Before the speed bump cover reaching the limiter: The dynamic equation of speed bump is derived from Eq. (22),

$$(M_b + M_e)\ddot{x}_b + C_b\dot{x}_b + K_b x_b - K_u(x_u - x_t) = F_p - F_g \tag{24}$$

(2) After the speed bump reach its limiter: As $\dot{x}_b = 0$, the dynamic equation of speed bump is switched to the following equation according to Eq. (21)

$$M_b\ddot{x}_b + K_b x_{b\max} - K_u(x_u - x_t) = F_p - F_g \tag{25}$$

(3) Rebounding process when vehicle tire rolling out of the speed bump cover: After the vehicle tire move out of the speed bump cover, the dynamic equation of the speed bump can be expresses as,

$$(M_b + M_b)\ddot{x}_b + C_b\dot{x}_b + K_b x_{b\max} = F_p \tag{26}$$

3.3 Harvested Electrical Power

As shown in Figure 3, the vibration of speed bump cover drives the down and up vibration of rack-pinion, which drive the shaft rotation of generator. The voltage, *U*, produced by generator is proportional to rotational velocity of generator, which can be describes as

$$U = k_g\omega \tag{27}$$

Where K_g is the voltage constant of the generator and ω is rotational velocity of generator, which can be calculated by the rack velocity, the same as the velocity of speed bump cover of $\dot{x}_b$ due to the hard connection of speed bump connector,

$$\omega = \frac{n\dot{x}_b}{r} \tag{28}$$

Here, *n* is the gear ratio of gear box and *r* is the radius of the pinion gear. Substitute Eq. (29) into Eq. (28), the harvested electrical voltage is

$$U = k_g\frac{n\dot{x}_b}{r} \tag{29}$$

When the external electrical load R_e is connected to the output of generator, electrical current will be produced in the close circuit with the internal resistance of the generator R_i and the external load resistance of R_e, then the output power can be expressed as

$$P = \frac{U^2}{(R_i + R_e)} = \frac{k_g^2 n^2 \dot{x}_b^2}{(r^2(R_i + R_e))} \tag{30}$$

The velocity of $\dot{x}_b$ can be calculated according to the dynamics analysis of the speed bump cover unit as introduced in section 3.2. Therefore, the harvested electrical power can be predicted according to Equation (31). Since external resistance can vary with voltage and current, a fixed value of external resistance of around 10.5 ohm has been assumed to get the electrical damping for the simplification of simulation. The motor parameters can be found in the website [13]. Point to be noted here is the external and internal resistance should be matched to get the maximum power output although this hasn't been discussed in simulation section. Simulation has been done for the validation our proposed design.

4 SIMULATION AND EXPERIMENTAL ANALYSIS OF SBEH PERFORMANCE AND ITS INTERACTION WITH VEHICLE

Simulation analysis is carried out to solve the numerical solution to the interaction models of SBEH and vehicle introduced in Section 3 by using commercial software, MATLAB. A vehicle parameter of class C type sedan in reference [5] has been adopted into the vehicle model. The parameters of SBEH model are setup according to the fabricated prototype. The necessary parameters are listed in Table 1.

Radius of Pinion Gear	R	0.0254	m
Sprung Mass	M_s	1527	kg
Un-Sprung Mass	M_u	200	kg
Speed Bump Mass	M_b	150	kg
Equivalent mass	M_e	620	kg
Total Mass (Speed bump and equivalent mass)	(M_b+M_e)	770	kg
Suspension Stiffness	K_s	60000	N/m
Tire stiffness	K_s	440000	N/m
Speed bump stiffness	K_b	130000	N/m
Suspension damping coefficient	C_s	7000	$N\text{-}s/m$
SBEH electrical damping coefficient	C_e	400	$N\text{-}s/m$
Gravitational constant	g	9.8	m/s^2
Gear Ratio	n	50 to 1	

Table 1. Axle vehicle and SBEH parameters

4.1 Dynamics performance simulation analysis of SBEH and vehicle

Dynamic performance of SBEH and the passing vehicle with and without energy harvester are conducted under the initial condition with vehicle speed at 5 km/h and 10 km/h. The displacement performance of the speed bump cover, the un-sprung mass, car body mass and the movable displacement on contacnt point between the tire and speed bump profile are illustrated in Figure 7, 8 and 9 for various speeds.

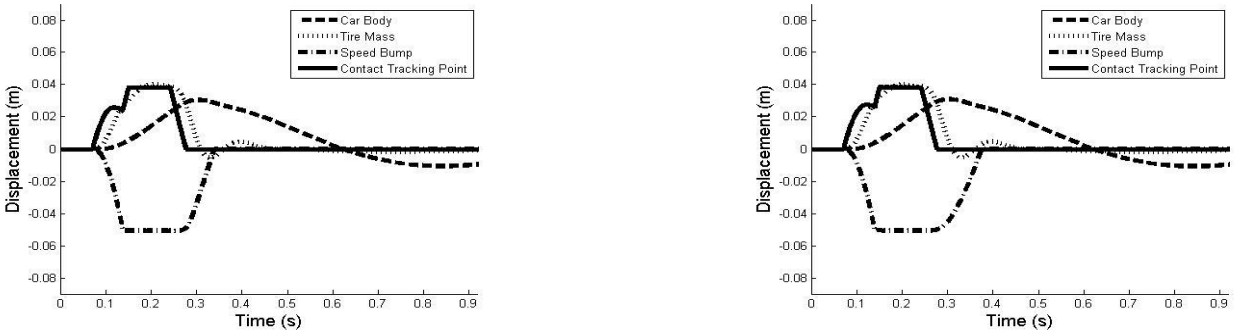

Figure 7. Simulated displacements under the vehicle speed at 5 km/h/. Left- SBEH model with MMR. Right- without MMR

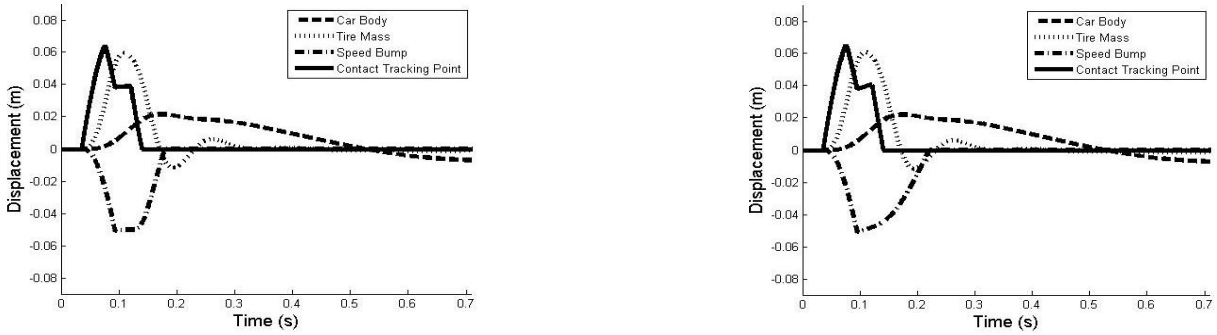

Figure 8. Simulated displacements under the vehicle speed at 10 km/h/. Left- SBEH model with MMR. Right- without MMR

The dynamics of the harvester and the vehicle is quite apparent in both the cases i.e. MMR and traditional damper (non MMR). In figure 8 and 9, we can see the car body, tire mass and the speed bump displacements under different velocities. At 10 km/h, the rate of vehicle climbing up the cover is higher than the rate of displacement of the cover. So the vehicle reaches the tip before the speed bump could touch its bottim limit. The flat line of the speed bump further represents the restricted movement till the vehicle is over the cover. At that time, the harvester dynamics disengages itself with the speed bump dynamics and hence we can retrieve more power which is discussed later in this section. As soon as the vehicle starts to go down the slope, speed bump starts to recover its original position and at around 0.2 sec with a faster velocity as compared to the non MMR case since the shaft is still running and system seems to be disengaged. Later it touches the upper hard stop and then stays stationary after that. During the process, vehicle body and the tire vibrate with the frequency about 10 Hz and 1 Hz, which meet the nature frequency performance of sprung and unsprung systems.

The simulated harvested electrical power under the vehicle speed at 5km/h and 10km/h are demonstrated too in Figure 9, and 10, which shows the difference between potential power generation using MMR mechanism and with the traditional harvesting method modelled with viscous damping.

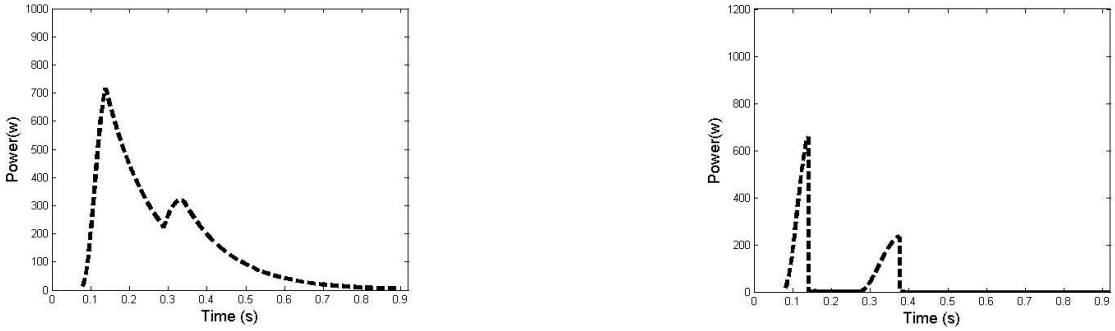

Figure 9. Simulated power under the vehicle speed at 5 km/h/. Left- SBEH model with MMR. Right- without MMR

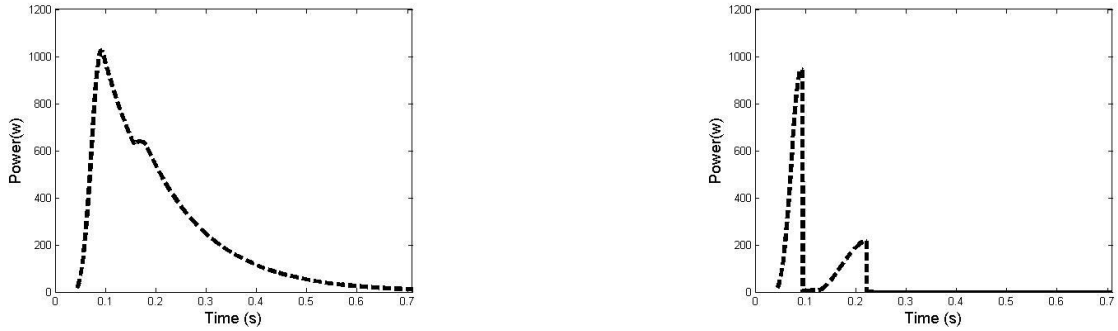

Figure 10. Simulated power under the vehicle speed at 10 km/h/. Left- SBEH model with MMR. Right- without MMR

From the power curves, we can clearly figure out the difference between the traditional damper and MMR system power output: the generator in MMR based design continues rotating and producing electricity when the speed bump cover reaches the stops Comparing the curves, we see that the area under the curves over the time in traditional deisgn (right side)of Figure 9,and 10, is much lesser, about 5 times, than the area in the corresponding MMR case (left sides) which indicates that more kinetic energy is recovered by MMR harvesters. Larger the area means more the energy has been converted into electricity. With the increase in velocity of the vehicle, area under the curve is getting larger in the MMR case which means there is more potential to transmit the kinematic energy into electricity using the MMR based harvesting mechanism.

The average power we get by MMR is also higher than that of non MMR case. This clearly indicates the advantages of MMR over any traditional harvesting mechanism.

4.2 In-field Test of SBEH Prototype

The SBEH prototype is tested by driving a vehicle to pass by on a wood trial. The harvested electrical energy from output of the generator is measured, as shown in Figure 13 There are two power peaks when one axle of the vehicle passing by the speed bump. The first large one is the energy harvested when speed bump is pressed down and the second peak is the harvested energy when the speed bump is rebounded up to its balance position. The largest peak power is about 200 watts.

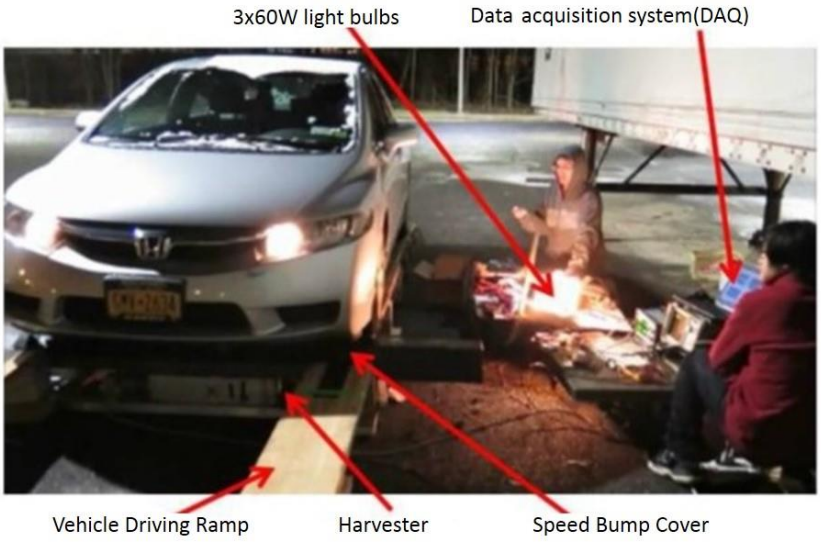

Figure 11. In field test of the SBEH.

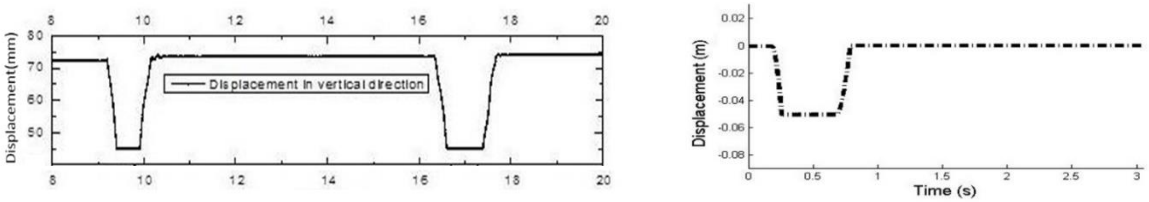

(a) Measured displacement of the speed bump cover (b) Simulated displacement of the speed bump cover

Figure 12. Comparison between measured and simulated displacements of the speed bump cover

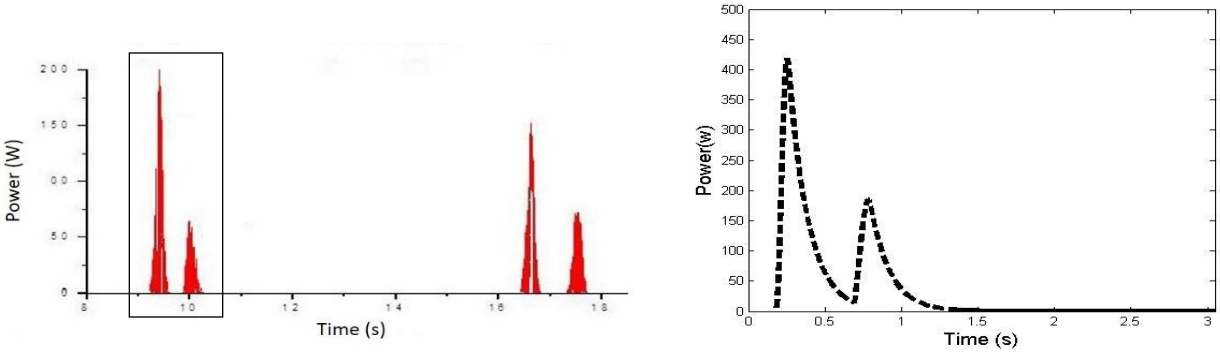

(a) Measured power from SBEH (b) Simulated power from SBEH

Figure 13. Comparision between measured and simulated electrical power output

Figure 12 illustrates the comparison of displacement between measured and simulated displacement of the speed bump cover. On the right (b), the simulated displacement contour and the duration of an axle of vehicle passing through the speed bump is similar to that of the measured results, which verifies the effectiveness of the proposed modeling approach of SBEH and its interaction with vehicle.

5 CONCLUSIONS

An effective design of energy harvesting speed bump is proposed. A prototype and in-field test by driving a vehicle passing by are investigated. High power up to 200 W in one phase out of three-phase generator can be achieved, which is much higher than the similar research in the literature. Modeling of the speed bump energy harvester and its interaction with the vehicle model are also explored. The simulation of dynamic performance and the predicted electrical energy harvesting when a vehicle passing by the speed bump energy harvester is carried out and compared with experimental results, which validate the effectiveness of the proposed design.. By comparing areas under the curve of power generated by MMR based harvester and the traditional electromagnetic harvester, we find that MMR based harvester generates about 4-5 times more energy, which demonstrates it advantages over traditional one for energy harvesting from the pulse-like excitations. The presented novel speed bump energy harvester and it compact structure can conveniently replace the existing traditional speed bumps with less impact to the dynamics of the passing vehicles.

The proposed speed bump energy harvester.is expected to provide sufficient electricity for many road side devices like signs, monitoring sensor and so on, which provide a cost-efficient energy source to supply electricity to intelligent transportation system especially in the areas where power grid cannot be accessed economically.

6 ACKNOWLEDGEMENT

The authors appreciate the partial funding support from SUNY Sustainability Fund. We also thank the students who were involved in design and testing, including Shifeng Yu, Shubin Chen, Shaoxu Xin, Shuyu Wang, and Changming Zou. Special thanks to machinists George Luhrs, Henry Honigman, and Joe.

REFERENCES

[1] E. Khorshid, F. Alkalby, and H. Kamal, “Measurement of whole-body vibration exposure from speed control humps,” J. Sound Vib., vol. 304, no. 3–5, 640–659, (2007).

[2] “Section 5 - Effect of Speed Bumps on Traffic Crashes | Traffic Calming Studies and Reports | The City of Portland, Oregon.” [Online]. Available: http://www.portlandoregon.gov/transportation/35934?a=85425. [Accessed: 09-Feb-2015].

[3] H. Ansari Ardeh, M. Shariatpanahi, and M. N. Bahrami, “Multiobjective shape optimization of speed humps,” Struct. Multidiscip. Optim., vol. 37, no. 2, 203–214, (2008).

[4] S. Arabia, “dynamic considerations of speed control humps (a) Hump profile,” vol. I, no. 4, 291–302, (1982).

[5] D. Garcia-Pozuelo, A. Gauchia, E. Olmeda, and V. Diaz, “Bump Modeling and Vehicle Vertical Dynamics Prediction,” Adv. Mech. Eng., vol. 2014,1–10, (2014).

[6] P. Taylor, T. Abiola, O. Salau, A. O. Adeyefa, and S. A. Oke, “Vehicle speed control using road bumps,” Transport, Vol XIX, No 3, 130–136, (2014)
[7] D. Chambers, “final project report assessment of piezoelectric materials for roadway energy Cost of Energy and Demonstration Roadmap,” (2014).
[8] “Piezoelectric Roads in California.” <http://large.stanford.edu/courses/2012/ph240/garland1/.>(09-Feb-2015).
[9] S. Andriopoulou, “A review on energy harvesting from roads.,” , 1–39, (2012).
[10] S. Priya, and D. Inman, "Energy harvesting technologies",Vol. 21, Springer, New York, (2009)
[11] J. Wang, T. Lin, and L. Zuo, “High Efficiency Electromagnetic Energy Harvester for Railroad Application,” ASME ASME 2013 International Design Engineering Technical Conferences, IDETC2013-12770. 1–10, (2013).
[12] R. N. Jazar, "Vehicle Dynamics: Theory and Applications", Springer, New York, 931 – 977,(2008)
[13] BLY34 - Brushless DC Motors. <https://www.anaheimautomation.com/products/brushless/brushless-motor-item.php?sID=150&pt=i&tID=96&cID=22>